

## Molecular model for carbon dioxide optimized to vapor-liquid equilibria

Thorsten Merker,<sup>1</sup> Cemal Engin,<sup>1</sup> Jadran Vrabec,<sup>2</sup> and Hans Hasse<sup>1,a)</sup>

<sup>1</sup>Laboratory of Engineering Thermodynamics, University of Kaiserslautern, 67633 Kaiserslautern, Germany

<sup>2</sup>Thermodynamics and Energy Technology, University of Paderborn, 33098 Paderborn, Germany

(Received 19 January 2010; accepted 5 May 2010; published online 21 June 2010)

A molecular model for carbon dioxide is presented, and the parameters of the Lennard-Jones sites, the bond length, and the quadrupole moment are optimized to experimental vapor-liquid equilibrium data. The resulting molecular model shows mean unsigned deviations to the experiment over the whole temperature range from triple point to critical point of 0.4% in saturated liquid density, 1.8% in vapor pressure, and 8.1% in enthalpy of vaporization. The molecular model is assessed by comparing predicted thermophysical properties with experimental data and a reference equation of state for a large part of the fluid region. The average deviations for density and residual enthalpy are 4.5% and 1.7%, respectively. The model is also capable to predict the radial distribution function, the second virial coefficient, and transport properties, the average deviations of the latter are 12%. © 2010 American Institute of Physics. [doi:10.1063/1.3434530]

### I. INTRODUCTION

Carbon dioxide is of great interest for our planet. It plays a central role in the green house effect and thus in global warming. Therefore, it is essential to reduce carbon dioxide emissions, e.g., via post combustion carbon dioxide capture in power plants.<sup>1</sup> In the chemical industry, it gains importance too, as it is increasingly used as an innovative reaction medium in its supercritical state.<sup>2</sup>

Molecular modeling and simulation is a modern approach for the prediction of thermophysical properties of pure fluids and mixtures, both in research and industry. This is due to several reasons. First, the predictive power of molecular models is superior to classical methods as it allows for results with high accuracy for a wide range of states. Second, a given molecular model provides access to the full variety of thermophysical properties, such as structural, thermal, caloric, transport, or phase equilibrium data. Finally, through the advent of cheaply available powerful computing infrastructure, reasonable execution times for molecular simulations can be achieved which are of crucial importance for industrial applications.

For carbon dioxide, several molecular models are available in the literature.<sup>3–14</sup> While earlier models,<sup>3–6</sup> such as the three center Lennard-Jones (3CLJ) plus point quadrupole (3CLJQ) model by Murthy *et al.*,<sup>3</sup> were parametrized on the basis of a few experimental data points for second virial coefficient or lattice energy, the two center Lennard-Jones plus point quadrupole (2CLJQ) model by Möller and Fischer<sup>7</sup> was the first which was parametrized using vapor-liquid equilibrium (VLE) data. It was followed by the 3CLJ plus point charges elementary physical model 2 (EPM2) by Harris and Yung,<sup>8</sup> where the main interest was the accurate description of the critical point. Bukowski *et al.*<sup>9</sup> and Bock *et*

*al.*<sup>10</sup> employed *ab initio* calculations to parametrize their five site models with complex pair potentials; however, Bratschi *et al.*<sup>15</sup> showed that these models are not able to accurately predict VLE properties. Potoff and Siepmann<sup>11</sup> optimized their 3CLJ plus point charges model to reproduce the VLE of the binary mixture carbon dioxide with propane. Vrabec *et al.*<sup>12</sup> published a readjusted version of the model by Möller and Fischer,<sup>7</sup> which shows a very good agreement for the VLE properties, but as it is a 2CLJQ model, the structure of the molecule is oversimplified. Zhang and Duan<sup>13</sup> published a 3CLJ plus point charges model claiming excellent results for VLE, structural, and transport properties. However, upon closer inspection, the VLE description of the model by Zhang and Duan<sup>13</sup> shows large deviations, especially for the vapor pressure and the saturated vapor density, being around 18% and 17%,<sup>16,17</sup> respectively. Recently, Zhu *et al.*<sup>14</sup> published a fully flexible 3CLJ plus point charges model, but unfortunately no VLE data were presented.

None of these models is able to describe the pure substance VLE very accurately and at the same time represent the physical structure appropriately. Most of the 3CLJ plus point charges models<sup>8,11,13,14</sup> were optimized to reproduce thermophysical properties, such as the critical point<sup>8</sup> or VLE of binary mixtures,<sup>11</sup> but not for the very accurate description of the pure component VLE over the whole temperature range from triple point to critical point. The 2CLJQ models<sup>7,12</sup> show a very good agreement for the VLE properties, but they are oversimplifying the molecular structure. Therefore, a rigid 3CLJQ model is proposed here to achieve both. An equivalent model, considering the internal degrees of freedom and describing the quadrupole by three point charges, is provided as well. Note that the rigid version requires roughly 30% less execution time during molecular simulation.

The paper is structured as follows. First, the new rigid carbon dioxide model is presented and the VLE properties are compared to models from the literature. Second, predictions of the second virial coefficient, transport properties,

<sup>a)</sup>Author to whom correspondence should be addressed. Tel.: +49-631/205-3497. FAX: +49-631/205-3835. Electronic mail: hans.hasse@mv.uni-kl.de.

and structural properties are made and compared to experimental data. Third, the equivalent flexible model with point charges is presented. Finally, the results are discussed and a conclusion is drawn.

## II. MOLECULAR MODEL

As a modeling *ansatz*, three LJ sites, representing the repulsive and dispersive interactions of the individual atoms, and a superimposed point quadrupole site were chosen. To define the model geometry, the nucleus positions were calculated by quantum chemistry, using the software package GAMESS (US).<sup>18</sup> A geometry optimization was performed on the Hartree–Fock, i.e., self-consistent field, level using the basis set 6-31G, which is a split-valence orbital basis set without polarizable terms. The nucleus positions from this *ab initio* calculation were used to initially specify the positions of the three LJ interaction sites. The resulting carbon-oxygen distance was  $r_{\text{CO}}=1.179$  Å. The point quadrupole was placed at the central carbon nucleus site and was aligned along the molecular axis.

To obtain the magnitude of the quadrupole, a subsequent quantum chemical calculation was performed. This was done on the Møller–Plesset 2 level using the polarizable basis set 6-311G(d,p) and the geometry from the previous step. It is widely known that polar moments of molecules in the gas phase significantly differ from those in the liquid phase. As preceding works<sup>12,19</sup> showed, molecular models yield better results for VLE properties when a “liquidlike” polar moment is applied. Therefore, the single carbon dioxide molecule was placed into a dielectric cavity (dielectric constant  $\epsilon=5$ ) utilizing the conductorlike screening model method<sup>20</sup> to mimic the liquid state. A quadrupole moment of  $Q=4.39$  DÅ ( $14.643 \times 10^{-40}$  Cm<sup>2</sup>) was obtained.

The parameters for the LJ sites were initially taken from Harris and Yung<sup>8</sup> and subsequently adjusted to saturated liquid density, vapor pressure, and enthalpy of vaporization from the reference equation of state (EOS) by Span and Wagner,<sup>21</sup> which is recommended by the National Institute of Standards and Technology.<sup>22</sup> The dominant LJ parameters are those representing the oxygen atoms as they have an eightfold stronger dispersive energy than the carbon LJ site. Furthermore, the carbon atom is partially shielded by the oxygen atoms. The parameter optimization was performed using a Newton scheme as proposed by Stoll.<sup>23</sup> The details are similar to those reported by Eckl *et al.*<sup>24</sup> and are not repeated here. VLE simulations were made with the grand equilibrium method;<sup>25</sup> technical simulation details are given in the Appendix.

During the optimization, it was necessary to adjust the carbon-oxygen distance and the quadrupole moment. The bond length between the carbon and the oxygen sites was increased by 8% and the quadrupole moment was decreased by 8%. The parameters of the final model are given in Table I.

## III. VLE

The present carbon dioxide model is compared with respect to VLE data to the EOS by Span and Wagner<sup>21</sup> and to

TABLE I. Parameters of the rigid carbon dioxide model.

$\sigma_{\text{C}}$ (Å)	$\epsilon_{\text{C}}/k_{\text{B}}$ (K)	$\sigma_{\text{O}}$ (Å)	$\epsilon_{\text{O}}/k_{\text{B}}$ (K)	$Q$ (DÅ)	$r_{\text{CO}}$ (Å)
2.8137	12.3724	2.9755	100.493	4.0739	1.2869

four molecular models from the literature: the 3CLJ plus point charges EPM2 model by Harris and Yung,<sup>8</sup> the 3CLJ plus point charges model by Zhang and Duan,<sup>13</sup> and the 2CLJQ models by Möller and Fischer<sup>7</sup> and Vrabec *et al.*<sup>12</sup> The results are presented in Figs. 1–3. A relative deviation plot and numerical results for the new carbon dioxide model are given in the supplementary material.<sup>26</sup>

Generally, the agreement between the new carbon dioxide model and the reference EOS (Ref. 21) is very satisfying. The mean unsigned errors in saturated vapor pressure, liquid density, and enthalpy of vaporization are 1.8%, 0.4%, and 8.1%, respectively, in the temperature range from 220 to 300 K, which is about 70%–98% of the critical temperature. Note that the triple point temperature is 217 K.<sup>21</sup> The critical temperature, density, and vapor pressure compare very favorably with the EOS (numbers in parentheses):  $T_{\text{c}}=304$  (304.13) K,  $\rho_{\text{c}}=10.6$  (10.625) mol/l, and  $p_{\text{c}}=7.4$  (7.377) MPa. Critical values of temperature, density, and vapor pressure for the new carbon dioxide model were derived following the procedure proposed by Lotfi *et al.*<sup>27</sup>

In comparison with the other molecular models from the literature, the present model is equivalent for the vapor pressure with the models by Möller and Fischer<sup>7</sup> and by Vrabec *et al.*<sup>12</sup> The other models, i.e., EPM2 (Ref. 8) and Zhang and Duan<sup>13</sup> overpredict the vapor pressure by around 10%, and 15%, respectively.

Apart from EPM2,<sup>8</sup> all models are within 1% of the reference EOS (Ref. 21) for the saturated liquid density between 220 and 290 K. Above 290 K, the present model and the one by Vrabec *et al.*<sup>12</sup> overpredict the saturated liquid density with a maximum of around 5% and 6%, respectively. Simulations near the critical point are quite challenging,

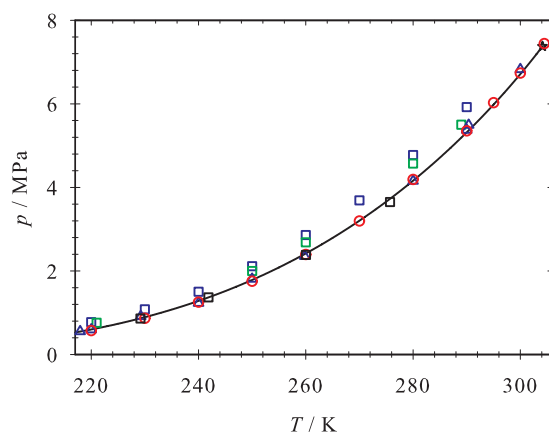


FIG. 1. Vapor pressure. Simulation results: (○, red) this work, (□, green) EPM2 (Ref. 8), (△, blue) Vrabec *et al.* (Ref. 12), (□, blue) Zhang and Duan (Refs. 13 and 16), (□, black) Möller and Fischer (Ref. 7), (—) EOS (Ref. 21), and ★ critical point (Ref. 21).

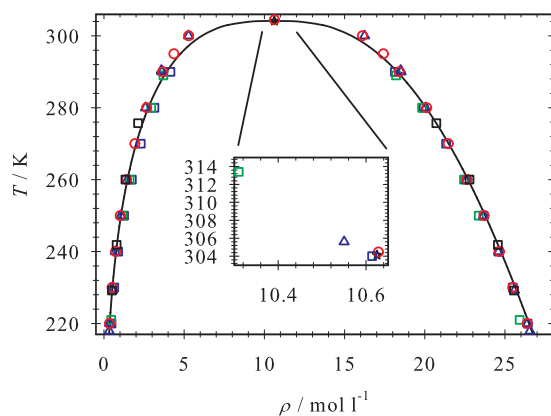


FIG. 2. Saturated densities. Simulation results: (○, red) this work, (□, green) EPM2 (Ref. 8), (△, blue) Vrabec *et al.* (Ref. 12), (□, blue) Zhang and Duan (Refs. 13 and 16), (□, black) Möller and Fischer (Ref. 7), (—) EOS (Ref. 21), and ★ critical point (Ref. 21). The inset is a magnified view of the critical point.

which is reflected by the increasing statistical uncertainties. For the other models, no VLE data are available for temperatures above 290 K.

The saturated vapor density is overpredicted by EPM2 (Ref. 8) and Zhang and Duan<sup>13</sup> by around 10% and 15%, respectively, which is in line with the vapor pressure deviations. Again, the present model is equivalent with the models by Möller and Fischer<sup>7</sup> and by Vrabec *et al.*<sup>12</sup> These models underpredict the vapor density by around 5% on average. The present model and the model by Vrabec *et al.*<sup>12</sup> deviate from the experimental data for the saturated vapor density above 290 K, whereas the model by Möller and Fischer<sup>7</sup> deviates already above 260 K.

For the enthalpy of vaporization, the EPM2,<sup>8</sup> Zhang and Duan,<sup>13</sup> and Möller and Fischer<sup>7</sup> models underpredict the enthalpy of vaporization by around 2%, 5%, and 10%, respectively. The present model and the one by Vrabec *et al.*<sup>12</sup> overpredict the enthalpy of vaporization between 220 and 290 K by around 9% and 6%, respectively.

#### IV. HOMOGENEOUS REGION

An important technical application of supercritical carbon dioxide is its use as an innovative reaction medium.

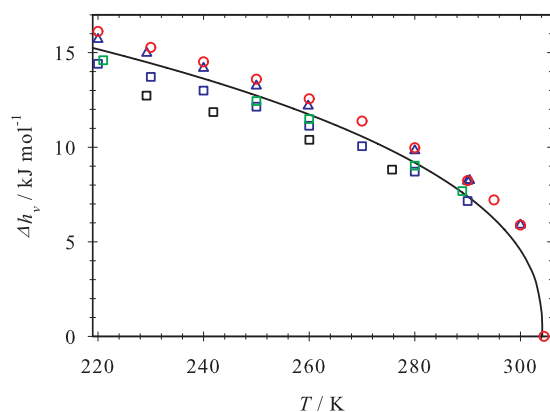


FIG. 3. Enthalpy of vaporization. Simulation results: (○, red) this work, (□, green) EPM2 (Ref. 8), (△, blue) Vrabec *et al.* (Ref. 12), (□, blue) Zhang and Duan (Refs. 13 and 16), (□, black) Möller and Fischer (Ref. 7), and (—) EOS (Ref. 21).

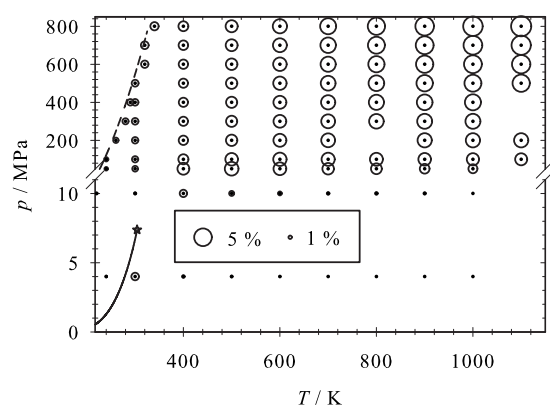


FIG. 4. Relative deviations for the density between simulation data and a reference EOS (Ref. 21) ( $\delta\rho = (\rho_{\text{sim}} - \rho_{\text{EOS}}) / \rho_{\text{EOS}}$ ) in the homogeneous fluid region: (○) this work, (—) vapor pressure curve (Ref. 21), and (---) melting line (Ref. 21). The size of the bubbles indicates the magnitude of the relative deviations.

Thus, to describe the properties of mixtures containing supercritical carbon dioxide, it is essential to cover the homogeneous region accurately. Thermal and caloric properties were predicted for the homogeneous liquid, vapor, and supercritical region. In total around 100 state points were studied, covering nearly the whole range of applicability of the reference EOS (Ref. 21) up to 1100 K and 800 MPa. Figure 4 shows the relative deviations between simulation and reference EOS (Ref. 21) for the density. Deviations are usually below 1% for vapor and liquid states. For the supercritical fluid state in the high pressure region, the deviations are higher, being around 5% with a maximum deviation of 6.8%.

The relative deviations for the residual enthalpy between simulation and reference EOS (Ref. 21) are shown in Fig. 5. Here, the deviations are maximal at low temperatures (up to 10%), whereas the typical deviations are below 1% for the remaining states.

#### V. SECOND VIRIAL COEFFICIENT

The predicted second virial coefficient is compared to the reference EOS (Ref. 21) in Fig. 6. It was calculated by evaluating Mayer's  $f$ -function as reported by Eckl *et al.*<sup>24</sup>

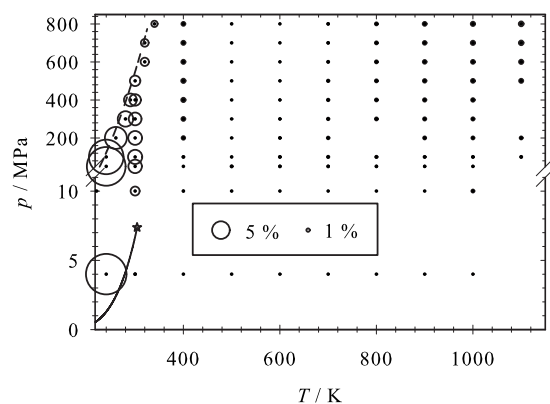


FIG. 5. Relative deviations for the residual enthalpy between simulation data and a reference EOS (Ref. 21) ( $\delta h^{\text{res}} = (h_{\text{sim}}^{\text{res}} - h_{\text{EOS}}^{\text{res}}) / h_{\text{EOS}}^{\text{res}}$ ) in the homogeneous fluid region: (○) this work, (—) vapor pressure curve (Ref. 21), and (---) melting line (Ref. 21). The size of the bubbles indicates the magnitude of the relative deviations.

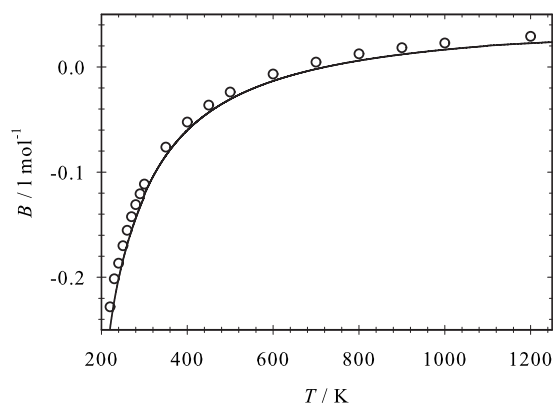


FIG. 6. Second virial coefficient: (○) this work and (—) EOS (Ref. 21).

The present model overestimates the second virial coefficient by only about 0.01 l/mol throughout the entire regarded temperature range from 200 to 1200 K. Numerical results are given in the supplementary material.<sup>26</sup>

## VI. STRUCTURAL PROPERTIES

Structural properties were studied on the basis of the atom-atom pair correlation functions  $g_{OO}(r)$ ,  $g_{CO}(r)$ , and  $g_{CC}(r)$ . The simulation results were compared to experimental neutron diffraction experiments by van Tricht *et al.*<sup>28</sup> Therefore, the neutron weighted pair correlation function  $g_m(r)$  was calculated by

$$g_m(r) = 0.403g_{OO}(r) + 0.464g_{CO}(r) + 0.133g_{CC}(r), \quad (1)$$

as reported by van Tricht *et al.*<sup>28</sup> In Fig. 7 (top), the present simulation results are compared to the EPM2 (Ref. 8) model

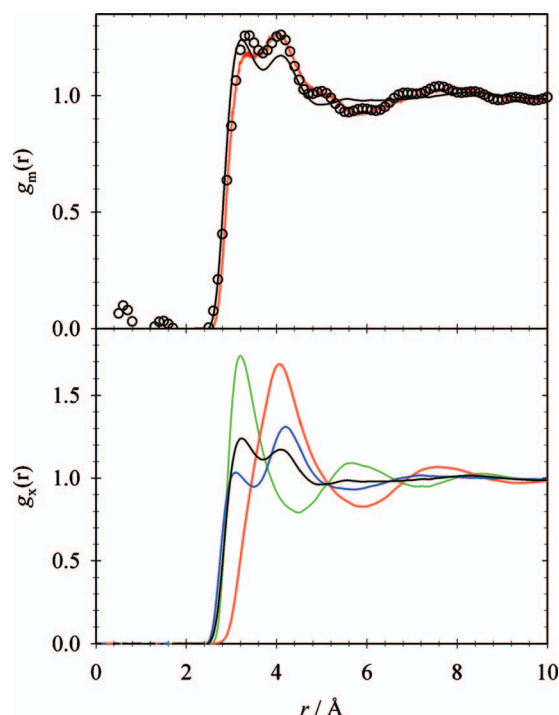


FIG. 7. Neutron weighted pair correlation function at 239 K and 1.45 MPa. Top: (○) experimental data (Ref. 28), (black line) this work, (red line) EPM2 (Ref. 8). Bottom (this work): (black line)  $g_m(r)$ , (green line)  $g_{OO}(r)$ , (red line)  $g_{CC}(r)$ , and (blue line)  $g_{CO}(r)$ .

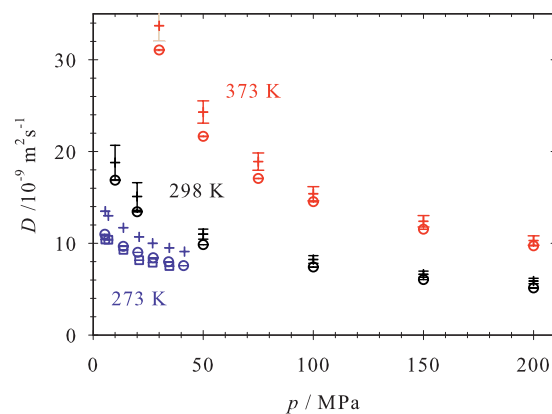


FIG. 8. Self-diffusion coefficient: (○) this work, (□) simulation data of Fernández *et al.* (Ref. 30) using the model of Vrabec *et al.* (Ref. 12), (+) experimental data partly including error bars (Refs. 31 and 32).

and to the experimental data<sup>28</sup> for a liquid state at 239 K and 1.45 MPa. The positions of the first two peaks from experiment and present carbon dioxide model agree excellently. The magnitudes of the second peak, however, are somewhat different. The first peak, which lies at around 3.2 Å, agrees well by the present molecular model, whereas the second peak at around 4 Å is underpredicted. van Tricht *et al.*<sup>28</sup> found a shoulder at around 5 Å, whereas the molecular model predicts a minimum at this distance. For distances larger than 5 Å, the weighted pair correlation function from molecular simulation is smoother than the experimental one. EPM2 (Ref. 8) shows an excellent agreement for the second peak and larger distances. However, the first peak is clearly underpredicted by EPM2.<sup>8</sup> The differences between the present carbon dioxide model and EPM2 (Ref. 8) are due to the higher  $\epsilon_C$  and lower  $\epsilon_O$  of EPM2,<sup>8</sup> which result in a higher peak for  $g_{CC}(r)$  and a lower peak for  $g_{OO}(r)$  (not shown here).

The simulated atom-atom pair correlation functions as well as the resulting neutron weighted pair correlation function are shown together in Fig. 7 (bottom). It can be seen that the first peak of  $g_m(r)$  is mainly due to  $g_{OO}(r)$  and  $g_{CO}(r)$ , whereas the second peak is due to  $g_{CC}(r)$  and  $g_{CO}(r)$ . Beyond 5 Å, the atom-atom pair correlation functions partly cancel each other out, which yields a rather constant  $g_m(r)$ . The numerical data for the partial atom-atom distribution functions are provided in the supplementary material.<sup>26</sup>

## VII. TRANSPORT PROPERTIES

Transport properties of carbon dioxide were obtained by equilibrium molecular dynamics (EMD) simulations following the Green–Kubo formalism. This approach allows for a direct relationship between a transport coefficient and the time integral of an autocorrelation function of a particular microscopic flux in a system in equilibrium. The calculation details are similar to those recently reported by Guevara *et al.*<sup>29</sup> and are not repeated here. Technical simulation details are given in the Appendix. The numerical results of the EMD simulations are listed in the supplemental material.<sup>26</sup>

In Fig. 8, the predicted self-diffusion coefficient is compared for three different temperatures to experimental data

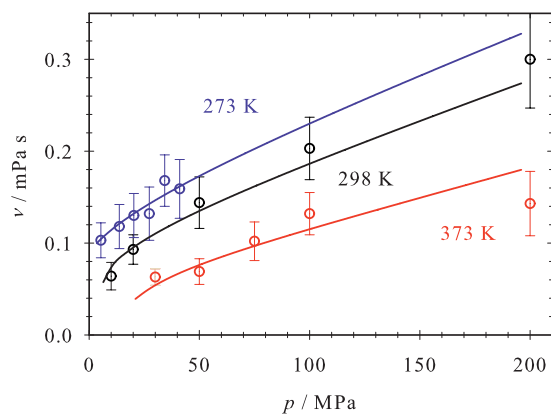


FIG. 9. Shear viscosity: (○) this work and (—) EOS (Ref. 33).

by Gross *et al.*<sup>31</sup> and Etesse *et al.*<sup>32</sup> and to predictions by Fernández *et al.*<sup>30</sup> for the temperature 273 K based on the model by Vrabec *et al.*<sup>12</sup> The present predictions underestimate the experiment by around 10%. Except for the lowest temperature, where no uncertainties are given in the literature, the predictions are close to the error bars of the experiment. Compared to the 2CLJQ model by Vrabec *et al.*,<sup>12</sup> the present model shows some improvement in the prediction of the self-diffusion coefficient.

The predictions for the shear viscosity are compared to the EOS by Fenghour *et al.*<sup>33</sup> for three temperatures in Fig. 9. The simulation data are in good agreement with the EOS,<sup>33</sup> being throughout within the simulation uncertainties.

The thermal conductivity was also predicted by EMD simulation. In Fig. 10, these data are compared to the EOS by Vesovic *et al.*<sup>34</sup> for three temperatures. The high statistical uncertainties are due to the strongly interacting molecules at high pressures, causing long time behaviors of the thermal conductivity autocorrelation function. As EMD is not best suited for determining the thermal conductivity, non-EMD (NEMD) simulation<sup>35</sup> should yield statistically more sound data at these state points. Nevertheless, a sufficient accuracy for a first assessment was achieved. The predictions for the thermal conductivity agree almost throughout within their (large) statistical uncertainties with the EOS.<sup>34</sup>

Recently, Nieto-Draghi *et al.*<sup>36</sup> published predictions of the transport properties on the basis of the EPM2 (Ref. 8) model. They used the Einstein relations for the shear viscos-

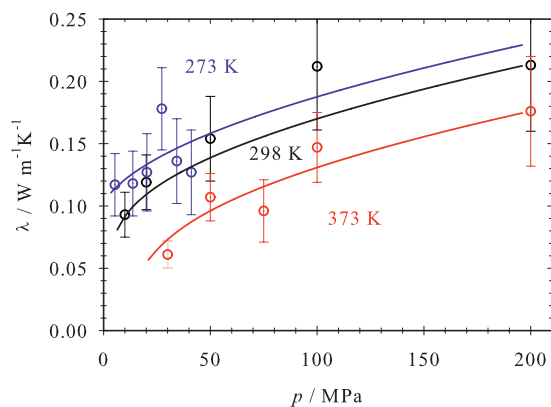


FIG. 10. Thermal conductivity: (○) this work and (—) EOS (Ref. 34).

ity and NEMD simulation for the thermal conductivity. Average deviations for shear viscosity and thermal conductivity were found to be 9% and 22%, which is in the same range as with the new molecular model.

## VIII. CARBON DIOXIDE MODEL WITH INTERNAL DEGREES OF FREEDOM

As many molecular simulation programs<sup>37–39</sup> do not feature point quadrupole interaction sites, an alternative version of the new model with point charges was developed. The point quadrupole was represented by three point charges, where the positive charge  $+2q$  is placed at the carbon LJ site and the two negative point charges  $-q$  are located at a distance  $\pm a$  on the molecular axis. The magnitude of the point charges  $q$  is related to the quadrupole moment  $Q$  by

$$Q = 2qa^2. \quad (2)$$

Schnabel<sup>40</sup> showed that good approximations can be achieved with a distance  $a=0.1$  Å. For the rigid model with point charges proposed here, a distance of  $a=0.2$  Å was chosen due to the large magnitude of the point charges which may lead to numerical difficulties during simulation. The magnitude of the resulting point charges is in this case  $q = 21.2 e$ .

Accompanying simulations with our own simulation program “ms2,” simulations for the rigid model with point charges were performed with the ERRINGTON code<sup>38</sup> to check for general use of the carbon dioxide model. No significant differences were found for the VLE properties between the point charge and the point quadrupole model, except for the enthalpy of vaporization (cf. Fig. 11).

For pure component VLE of small molecules like carbon dioxide, usually no or very small differences are found between rigid and flexible molecules, if only the LJ site arrangement is flexible but not the charges. Nonetheless, a flexible version of the new molecular model was developed here as well. Harmonic potentials were used for bond and angle stretching, using the parameters as introduced by Nieto-Draghi *et al.*<sup>36</sup> (cf. Table II). Note that the point charges themselves were chosen to have a rigid arrangement. The simulations were performed with the ERRINGTON code.<sup>38</sup> As expected, the flexible and the rigid models lead to the same VLE data (cf. Fig. 11).

## IX. CONCLUSION

The goal of this work was the development of a molecular model for carbon dioxide that accurately describes the VLE over the whole temperature range and at the same time represents the molecular structure appropriately. The model consists of three LJ sites and one quadrupole located in the center of mass. The parameters of the model were adjusted to VLE data. The results were compared to other models from the literature. The new model was found to be as good as the most accurate model by Vrabec *et al.*<sup>12</sup> regarding saturated densities and vapor pressure. For the enthalpy of vaporization, EPM2 was found to be the best one.

It seems that a better description of the vapor pressure is associated by an overestimation of the enthalpy of vaporiza-

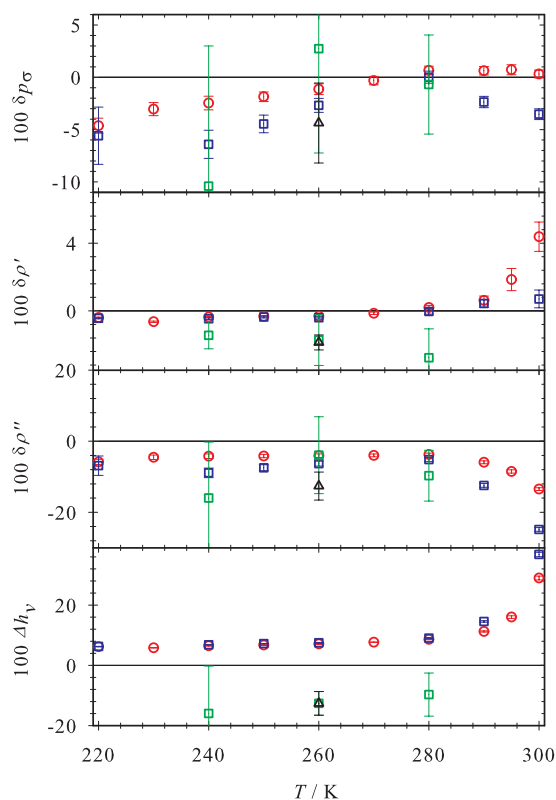


FIG. 11. Relative deviations of VLE properties between simulation data and a reference EOS (Ref. 21) ( $\delta z = (z_{\text{sim}} - z_{\text{EOS}}) / z_{\text{EOS}}$ ): (○, red) point quadrupole (*ms2*), (□, blue) point charge, rigid (*ms2*), (□, green) point charge, rigid (ERRINGTON code), and (△, black) point charge, flexible (ERRINGTON code). From top to bottom: vapor pressure, saturated liquid density, saturated vapor density, and enthalpy of vaporization.

tion and vice versa. During the model adjustment, it was not possible to better describe at the same time both properties. The adjustment of the carbon-oxygen distance and the quadrupole moment had no significant effect on this issue, but it improved the description of the saturated densities and the vapor pressure, especially at higher temperatures near the critical point. Thus, further investigations are needed.

The new model is capable to predict thermal and caloric properties over a large range of states. The second virial coefficient was predicted with an almost constant small offset compared to a reference EOS. The predicted neutron weighted radial distribution functions at a liquid state point is in good agreement with experimental neutron diffraction data. EMD simulations were performed to predict transport properties. The predictions of the self-diffusion coefficient on the basis of the new model show some improvement compared to the model by Vrabec *et al.*<sup>12</sup> and are in good agreement with experimental data. The predicted shear viscosity and thermal conductivity data are also in good agreement with EOS data.

TABLE II. Parameters for the new flexible carbon dioxide model. The distance between the LJ sites for carbon and oxygen is denoted by  $r_{\text{CO}}$  and the distance between the carbon LJ site and the oxygen point charges is denoted by  $r_{\text{Cq}}$ . The parameters  $k_r$  and  $k_\theta$  are the bond stretching and bond bending force constants, respectively, and were taken from Nieto-Draghi *et al.* (Ref. 36).

$\sigma_{\text{C}}$ (Å)	$\varepsilon_{\text{C}}/k_{\text{B}}$ (K)	$\sigma_{\text{O}}$ (Å)	$\varepsilon_{\text{O}}/k_{\text{B}}$ (K)	$r_{\text{CO}}$ (Å)	$q_{\text{C}}$ (e)	$q_{\text{O}}$ (e)	$r_{\text{Cq}}$ (Å)	$k_r$ (kJ mol <sup>-1</sup> Å <sup>-2</sup> )	$k_\theta$ (kJ mol <sup>-1</sup> rad <sup>-2</sup> )
2.8137	12.3724	2.9755	100.493	1.2869	21.2	-10.6	0.2	10 739.337	1236

For a more general use of the present carbon dioxide model, alternative versions with point charges instead of a point quadrupole and considering the internal degrees of freedom were provided. Regarding VLE properties, no significant differences were found between the different versions of the new model.

## ACKNOWLEDGMENTS

The authors gratefully acknowledge financial support by Deutsche Forschungsgemeinschaft, Collaborative Research Centre SFB 706 “Selective Catalytic Oxidations Using Molecular Oxygen.” The presented research was conducted under the auspices of the Boltzmann-Zuse Society of Computational Molecular Engineering (BZS). The simulations were performed on the national super computer NEC SX-8 at the High Performance Computing Centre Stuttgart (HLRS) under the grant MMHBF and on the HP XC4000 supercomputer at the Steinbruch Centre for Computing under the grant LAMO.

## APPENDIX: SIMULATION DETAILS

In this work, the grand equilibrium method<sup>25</sup> was used for VLE simulations. To determine the chemical potential in the liquid, gradual insertion<sup>41</sup> and Widom’s insertion method<sup>42</sup> were used. For low temperatures near the triple point, gradual insertion yields results with much lower statistical uncertainties than Widom’s method.

Widom’s method was applied in conjunction with molecular dynamics simulations in the isothermal-isobaric ( $NpT$ ) ensemble using isokinetic velocity scaling<sup>43</sup> and Anderson’s barostat.<sup>44</sup> There, the number of molecules was 1372 and the time step was 1 fs. The initial configuration was a face centered cubic lattice; the fluid was equilibrated over 60 000 time steps with the first 10 000 time steps in the canonical ( $NVT$ ) ensemble. The production run went over 400 000 time steps with a membrane mass of 10<sup>9</sup> kg/m<sup>4</sup>. Up to 5000 test molecules were inserted every production time step.

For gradual insertion, Monte Carlo simulations in the  $NpT$  ensemble were performed using 1372 molecules. Starting from a face centered cubic lattice, 15 000 Monte Carlo cycles were performed for equilibration with the first 5000 time steps in the  $NVT$  ensemble and 100 000 for production, each cycle containing 1372 displacement moves, 1372 rotation moves, and one volume move. Every 50 cycles, 13 720 fluctuating state change moves, 13 720 fluctuating particle translation/rotation moves, and 68 600 biased particle translation/rotation moves were performed to determine the chemical potential.

For the corresponding vapor, Monte Carlo simulations in the pseudo-grand-canonical (pseudo- $\mu VT$ ) ensemble were made. The simulation volume was adjusted to lead to an average number of 864 molecules in the vapor phase. After 10 000 initial  $NVT$  Monte Carlo cycles, starting from a face centered cubic lattice, 25 000 equilibration cycles in the pseudo- $\mu VT$  ensemble were performed. The length of the production run was 100 000 cycles. One cycle is defined here to be a number of attempts to displace and rotate molecules equal to the actual number of molecules plus three insertion and three deletion attempts.

The cutoff radius was set to at least 21 Å and a center of mass cutoff scheme was employed. LJ long-range interactions beyond the cutoff radius were corrected as proposed by Lustig.<sup>45</sup> The reaction field method<sup>43</sup> was used for the point charge model. Statistical uncertainties of the simulated values were estimated by a block averaging method.<sup>46</sup>

For the simulations in the homogeneous region, molecular dynamics simulations were made with the same technical parameters as used for the liquid runs during VLE calculation.

For the pair correlation functions molecular dynamics simulation runs were made with 1372 molecules. Intermolecular site-site distances were divided in 1000 slabs from 0 to 10 Å and averaged over 500 000 time steps.

The second virial coefficient was calculated by evaluating Mayer's  $f$ -function at 563 radii from 2 to 24 Å, averaging over 1000<sup>2</sup> random orientations at each radius. The random orientations were generated using a modified Monte Carlo scheme.<sup>47,48</sup> A cutoff correction was applied for distances larger than 24 Å for the LJ potential.<sup>43</sup> The electrostatic interactions need no long-range correction as they vanish by angle averaging.

EMD simulations for transport properties were made in two steps. In the first step, a short simulation in the  $NpT$  ensemble was performed at the specified temperature and pressure to calculate the respective density. In the second step, a  $NVT$  ensemble simulation was made at this temperature and density to determine the transport properties. The simulations were carried out in a cubic box with periodic boundary conditions containing 4000 molecules. In all EMD simulations, the integration time step was 1 fs. The cutoff radius was set to 21 Å. The simulations were equilibrated in the  $NVT$  ensemble over 50 000 time steps, followed by production runs of  $1 \times 10^6$  time steps. The sampling length of the autocorrelation functions was 17.5 ps.

Monte Carlo simulations with the ERRINGTON code<sup>38</sup> were performed in the  $NVT$  Gibbs ensemble<sup>49,50</sup> with a starting configuration of 800 molecules in the liquid box and 200 molecules in the vapor box. Both boxes were filled with the configurational bias growth method.  $8 \times 10^6$  Monte Carlo moves were performed with the first  $4 \times 10^6$  moves for equilibration and the remaining  $4 \times 10^6$  moves for production. The ratios of attempted moves were as follows: 1% volume exchange, 15% molecule exchange, 42% translations, and 42% rotations.

- <sup>1</sup>R. Notz, N. Aspiron, I. Clausen, and H. Hasse, *Chem. Eng. Res. Des.* **85**, 510 (2007).
- <sup>2</sup>W. Leitner, *Acc. Chem. Res.* **35**, 746 (2002).
- <sup>3</sup>C. S. Murthy, K. Singer, and I. R. McDonald, *Mol. Phys.* **44**, 135 (1981).
- <sup>4</sup>H. J. Böhm, C. Meissner, and R. Ahlrichs, *Mol. Phys.* **53**, 651 (1984).
- <sup>5</sup>S. B. Zhu and G. W. Robinson, *Comput. Phys. Commun.* **52**, 317 (1989).
- <sup>6</sup>R. D. Etters and B. Kuchta, *J. Chem. Phys.* **90**, 4537 (1989).
- <sup>7</sup>D. Möller and J. Fischer, *Fluid Phase Equilib.* **100**, 35 (1994).
- <sup>8</sup>J. G. Harris and K. H. Yung, *J. Chem. Phys.* **99**, 12021 (1995).
- <sup>9</sup>R. Bukowski, J. Sadlej, B. Jeziorski, P. Jankowski, K. Szalewicz, S. A. Kucharski, H. L. Williams, and B. M. Rice, *J. Chem. Phys.* **110**, 3785 (1999).
- <sup>10</sup>S. Bock, E. Bich, and E. Vogel, *Chem. Phys.* **257**, 147 (2000).
- <sup>11</sup>J. J. Potoff and J. I. Siepmann, *AIChE J.* **47**, 1676 (2001).
- <sup>12</sup>J. Vrabec, J. Stoll, and H. Hasse, *J. Phys. Chem. B* **105**, 12126 (2001).
- <sup>13</sup>Z. Zhang and Z. Duan, *J. Chem. Phys.* **122**, 214507 (2005).
- <sup>14</sup>A. Zhu, X. Zhang, Q. Liu, and Q. Zhang, *Chin. J. Chem. Eng.* **17**, 268 (2009).
- <sup>15</sup>C. Bratschi, H. Huber, and D. J. Searles, *J. Chem. Phys.* **126**, 164105 (2007).
- <sup>16</sup>T. Merker, J. Vrabec, and H. Hasse, *J. Chem. Phys.* **129**, 087101 (2008).
- <sup>17</sup>Z. Zhang and Z. Duan, *J. Chem. Phys.* **129**, 087102 (2008).
- <sup>18</sup>M. W. Schmidt, K. K. Baldrige, J. A. Boatz, S. T. Elbert, M. S. Gordon, J. H. Jensen, S. Koseki, N. Matsunaga, K. A. Nguyen, T. L. Windus, M. Dupuis, and J. A. Montgomery, Jr., *J. Comput. Chem.* **14**, 1347 (1993).
- <sup>19</sup>J. Stoll, J. Vrabec, and H. Hasse, *J. Chem. Phys.* **119**, 11396 (2003).
- <sup>20</sup>K. Baldrige and A. Klamt, *J. Chem. Phys.* **106**, 6622 (1997).
- <sup>21</sup>R. Span and W. Wagner, *J. Phys. Chem. Ref. Data* **25**, 1509 (1996).
- <sup>22</sup>National Institute of Standards and Technology.
- <sup>23</sup>J. Stoll, *Molecular Models for the Prediction of Thermophysical Properties of Pure Fluids and Mixtures* (VDI-Verlag, Düsseldorf, 2005).
- <sup>24</sup>B. Eckl, J. Vrabec, and H. Hasse, *Mol. Phys.* **106**, 1039 (2008).
- <sup>25</sup>J. Vrabec and H. Hasse, *Mol. Phys.* **100**, 3375 (2002).
- <sup>26</sup>See supplementary material at <http://dx.doi.org/10.1063/1.3434530> for numerical data and additional figures.
- <sup>27</sup>A. Lotfi, J. Vrabec, and J. Fischer, *Mol. Phys.* **76**, 1319 (1992).
- <sup>28</sup>J. B. van Tricht, H. Fredrikze, and J. van der Laan, *Mol. Phys.* **52**, 115 (1984).
- <sup>29</sup>G. Guevara-Carrion, C. Nieto-Draghi, J. Vrabec, and H. Hasse, *J. Phys. Chem. B* **112**, 16664 (2008).
- <sup>30</sup>G. A. Fernandez, J. Vrabec, and H. Hasse, *Int. J. Thermophys.* **26**, 1389 (2005).
- <sup>31</sup>T. Groß, J. Buchhauser, and H.-D. Lüdemann, *J. Chem. Phys.* **109**, 4518 (1998).
- <sup>32</sup>P. Etesse, J. A. Zega, and R. Kobayashi, *J. Chem. Phys.* **97**, 2022 (1992).
- <sup>33</sup>A. Fenghour, W. A. Wakeham, and V. Vesovic, *J. Phys. Chem. Ref. Data* **27**, 31 (1997).
- <sup>34</sup>V. Vesovic, W. A. Wakeham, G. A. Olchowy, J. V. Sengers, J. T. R. Watson, and J. Millat, *J. Phys. Chem. Ref. Data* **19**, 763 (1990).
- <sup>35</sup>F. Müller-Plathe, *J. Chem. Phys.* **106**, 6082 (1997).
- <sup>36</sup>C. Nieto-Draghi, T. de Bruin, J. Pérez-Pellitero, J. B. Avalos, and A. D. Mackie, *J. Chem. Phys.* **126**, 064509 (2007).
- <sup>37</sup>See <http://towhee.sourceforge.net> for the TOWHEE Monte Carlo molecular simulation code.
- <sup>38</sup>See <http://kea.princeton.edu/jerring/gibbs> the ERRINGTON Monte Carlo molecular simulation code.
- <sup>39</sup>B. Hess, C. Kutzner, D. van der Spoel, and E. Lindahl, *J. Chem. Theory Comput.* **4**, 435 (2008).
- <sup>40</sup>T. Schnabel, *Molecular Modeling and Simulation of Hydrogen Bonding Pure Fluids and Mixtures* (Logos, Berlin, 2008).
- <sup>41</sup>J. Vrabec, M. Kettler, and H. Hasse, *Chem. Phys. Lett.* **356**, 431 (2002).
- <sup>42</sup>B. Widom, *J. Chem. Phys.* **39**, 2808 (1963).
- <sup>43</sup>M. P. Allen and D. J. Tildesley, *Computer Simulation of Liquids* (Clarendon, Oxford, 1987).
- <sup>44</sup>H. C. Andersen, *J. Chem. Phys.* **72**, 2384 (1980).
- <sup>45</sup>R. Lustig, *Mol. Phys.* **65**, 175 (1988).
- <sup>46</sup>H. Flyvbjerg and H. G. Petersen, *J. Chem. Phys.* **91**, 461 (1989).
- <sup>47</sup>R. D. Mountain, *J. Phys. Chem. B* **109**, 13352 (2005).
- <sup>48</sup>B. Eckl, J. Vrabec, and H. Hasse, *Fluid Phase Equilib.* **274**, 16 (2008).
- <sup>49</sup>A. Z. Panagiotopoulos, *Mol. Phys.* **61**, 813 (1987).
- <sup>50</sup>A. Z. Panagiotopoulos, N. Quirke, M. R. Stapleton, and D. J. Tildesley, *Mol. Phys.* **63**, 527 (1988).